

Effect of Pat/Agave/Coir-Dust Reinforcement on the Mechanical and Moisture Properties of Epoxy Composites

Nashmi H. Alrasheedi 

Epoxy composites were reinforced with alkali (NaOH)-treated pat (jute) fibers, untreated agave fibers, and coir dust to improve mechanical and moisture resistance properties. Alkali treatment was applied to the pat fibers. Ten formulations (PA1–PA10) were fabricated by varying fiber proportions and evaluated for tensile, flexural, impact, hardness, interlaminar shear strength (ILSS), density, water absorption, and thickness swelling. Mechanical performance strongly depended on fiber composition and interfacial bonding. Tensile strength increased from 22 MPa (neat epoxy, PA10) to 44 MPa (PA3), while flexural strength ranged from 25 to 52 MPa, with PA3 showing superior performance. The highest impact strength (0.40 J), hardness (84 Shore D), and ILSS (9 MPa) were also observed for PA3, indicating efficient stress transfer. Moisture analysis showed minimum water absorption (10%) and thickness swelling (2.3%) for PA3. Density ranged between 1.20 and 1.36 g/cm³, suggesting that performance was governed mainly by interfacial interaction. Overall, PA3 (15% treated pat and 15% agave fiber) demonstrated the best balance of strength and environmental resistance. That formulation demonstrated the most balanced combination of mechanical strength, interlaminar integrity, and environmental resistance, highlighting the effectiveness of fiber reinforcement with coir dust for green epoxy composites.

DOI: 10.15376/biores.21.3.6174-6202

Keywords: Mechanical characterization; Sustainable composites; Mechanical testing; Water absorption behavior; Pat; Agave; Coir dust

Contact information: Department of Mechanical Engineering, College of Engineering, Imam Mohammad Ibn Saud Islamic University (IMSIU), Riyadh, 11432, Kingdom of Saudi Arabia;

* Corresponding author: nhrasheedi@imamu.edu.sa

INTRODUCTION

Natural fibers and fillers have attracted considerable interest in the composite industry because of their various benefits, such as renewability, biodegradability, and cost-effectiveness (Mittal and Chaudhary 2018; Ramasubbu *et al.* 2024). These characteristics render them exceptionally suited for the advancement of sustainable materials that correspond with worldwide initiatives aimed at minimizing environmental effects. Jute and agave fibers are notable for their exceptional strength, broad availability, and versatility among the many natural fibers (Karuppusamy *et al.* 2023). Both fibers have proven to be crucial elements in the advancement of composite materials, especially in areas where they are widely grown. Nonetheless, despite their benefits, the intrinsic hydrophilic characteristics of these fibers pose a significant challenge (Bhuvaneswari *et al.* 2022). This characteristic restricts their compatibility with hydrophobic polymer matrices, frequently

leading to inadequate interfacial bonding and diminished composite properties. Resolving this issue is essential for realizing the complete capabilities of natural fiber composites in both structural and functional applications (Kumar *et al.* 2022; Kar *et al.* 2024). Chemical treatments have proven to be effective solutions for improving the compatibility between natural fibers and polymer matrices. Among these, alkali treatment is a widely used and effective method (Mittal *et al.* 2016). This procedure entails subjecting the fibers to a NaOH solution, effectively eliminating impurities such as lignin, hemicellulose, and surface waxes. The elimination of these components enhances the surface smoothness of the fibers and introduces hydroxyl groups, which promote stronger interfacial bonding with the polymer matrix (Cisneros-López *et al.* 2017). Alongside enhancing mechanical properties, alkali treatment effectively decreases the hydrophilicity of fibers, thereby lessening their propensity to absorb moisture. The fibers are thus rendered more appropriate for applications in settings where maintaining dimensional stability is essential.

Jute fiber, which is commonly known as “golden fiber” because of its shiny and lustrous look, is among the most widely utilized natural fibers in the composite industry (Sathishkumar *et al.* 2014; Ayrilmis *et al.* 2024). This material originates from the bast or outer layer of the jute plant and consists mainly of cellulose, hemicellulose, and lignin. The material’s impressive tensile strength, reasonable elongation, and effective thermal insulation characteristics render it a compelling option for enhancing polymer composites. Jute is abundantly accessible in substantial amounts, especially in the nations of India and Bangladesh, where it is widely farmed (Ibrahim *et al.* 2016). Similarly, agave fiber, obtained from the leaves of the agave plant, is another natural fiber with considerable potential. Known for its high stiffness, strength, and resistance to microbial degradation, agave fiber has been increasingly used in composite applications. However, like jute, its hydrophilic nature necessitates chemical modification to improve its compatibility with polymer matrices (Vigneshwaran *et al.* 2020). In addition to natural fibers, fillers play a vital role in composite materials. Coir dust, a byproduct of coconut processing, is an example of an effective filler that has gained attention in recent years. Coir dust particles are derived from the monocarp or husk of coconuts and are primarily composed of lignin and cellulose (Govindarajan *et al.* 2024; Mahalingam 2024). This filler material offers several advantages, including low cost, high availability, and good thermal stability. When incorporated into composites, coir dust particles act as a reinforcing agent, enhancing mechanical properties such as stiffness and impact resistance. Additionally, their use contributes to the value-added utilization of agricultural waste, aligning with the principles of sustainability and circular economy (Dugvekar and Dixit 2022).

The combination of various natural fibers and fillers presents a valuable strategy for creating composites with customized characteristics. Combining fibers with complementary mechanical characteristics allows for a balanced outcome of strength, stiffness, and toughness in the final composite material (Praveena *et al.* 2022; Goutham *et al.* 2023). The incorporation of fillers, such as coir dust particles, significantly improves the performance of these hybrids by enhancing dimensional stability, lowering material costs, and boosting specific mechanical properties (Gurusamy *et al.* 2024). Nonetheless, the success of hybridization is influenced by various elements, such as the specific fibers and fillers employed, their ratios, and the bonding at the interface between the components.

This study analyzed the effects of hybridization using chemically modified jute (pat) and agave fibers mixed with coir dust particles in epoxy composites (Dharmaratne *et al.* 2021). The primary objective was to evaluate the mechanical performance and water absorption properties of these hybrid composites. The mechanical qualities, such as tensile

strength, compressive strength, flexural strength, hardness, and impact resistance, are critical determinants of the suitability of composites for structural applications (Kumar and Raja 2021). The behavior of water absorption provides critical insights into the environmental stability and durability of the composites, particularly in humid or wet situations. The use of chemically modified fibers into epoxy matrix has significantly improved the mechanical characteristics of composites. Alkali-treated jute and agave fibers have been found to exhibit better interfacial adhesion with the matrix, resulting in improved load transmission and mechanical performance (Chithra *et al.* 2024).

The incorporation of coir dust particles enhances the composite structure by effectively filling voids and serving as agents for stress transfer. The combined influence of fibers and fillers is anticipated to yield hybrid composites that exhibit enhanced properties when compared to those reinforced with only one type of fiber or filler (Badyankal *et al.* 2021). The absorption of water is a significant element that affects the long-term efficacy of natural fiber composites. Natural fibers that have not been treated exhibit a strong affinity for water, resulting in swelling, changes in dimensions, and a decline in mechanical properties as time progresses (Gupta and Ramkumar 2021). Chemical treatments such as alkali treatment can markedly decrease the water absorption capacity of fibers by eliminating hydrophilic components and diminishing the presence of free hydroxyl groups. The addition of coir dust particles, characterized by their lower hydrophilicity compared to untreated fibers, enhances the water resistance of the hybrid composites. Through a methodical examination of the water absorption characteristics of these materials, important understanding can be achieved regarding their appropriateness for use in humid or wet conditions (Aruchamy *et al.* 2025).

The possible uses of these hybrid composites are extensive and varied. In the construction sector, these materials serve as lightweight and durable options for panels, roofing, and flooring applications. In the automotive sector, there is an eco-friendly alternative to synthetic composites for both interior and exterior components (Manickaraj *et al.* 2024b). The advancement of these materials presents significant potential for consumer products, packaging, and various sectors where sustainability and performance are of paramount importance. While there are benefits to natural fiber composites, their broad implementation faces several obstacles. The differences in fiber properties, shaped by elements like plant species, growth conditions, and processing techniques, can result in variations in composite performance (Kumar *et al.* 2021). Furthermore, the affinity of natural fibers for moisture and their consequent sensitivity pose considerable challenges. Nonetheless, continuous exploration and progress in chemical treatments, hybridization techniques, and composite fabrication methods persist in tackling these challenges, facilitating the wider use of natural fiber composites (Thangavel *et al.* 2024).

In natural fiber composites, fiber length and alignment critically influence mechanical performance. Unlike thermoplastic extrusion, epoxy processing (hand lay-up/compression molding) preserves fiber length and orientation, enhancing stress transfer and strength (Pandiarajan *et al.* 2025). Although epoxy is more brittle and costly, this approach allows effective reinforcement with hybrid fibers such as pat and agave combined with coir dust, improving mechanical and moisture-related properties in high-performance green composites (Gunti *et al.* 2018).

This study systematically evaluated the mechanical properties and water absorption behavior of hybrid composites reinforced with chemically modified jute (pat) and agave fibers, in addition to coir dust particles. The goal was to enhance existing knowledge on sustainable composite materials and establish a basis for their use across different sectors

(Praveen Kumar and Nalla Mohamed 2018). This study illustrates how chemical modification and hybridization can significantly improve composite performance, with the goal of advancing the creation of sustainable materials that align with contemporary engineering and design requirements (Thirumalaisamy *et al.* 2023).

EXPERIMENTAL

Fibers

The fibers used in this study were pat (jute) and agave. Pat fiber is strong, flexible, and widely available, making it suitable for composite applications. Agave fibers are stiff, durable, and resistant to microbial degradation, providing additional strength to composites (Palanisamy *et al.* 2022a; Manickaraj *et al.* 2024c). The fibers were collected from Amman Impex, Pollachi, Tamil Nadu, India. Figure 1 shows various fibers.



Fig. 1. a: Pat Fiber; b: Agave Fiber



Fig. 2. Coir dust fillers

Filler

Coir dust particles were used as a filler. Coir dust is a byproduct of coconut processing, composed of cellulose and lignin. It is an affordable, eco-friendly material that enhances the composite's stiffness, impact resistance, and water absorption resistance (Del Campo *et al.* 2020). The fillers were collected from local village in Pollachi, Tamil Nadu, India. Figure 2 shows the coir dust fillers.

Matrix

The matrix material consisted of epoxy resin blended with an appropriate hardener. Epoxy resin provides outstanding mechanical properties, exceptional chemical resistance, and robust adhesion to natural fibers, rendering it highly suitable for reinforcing composites (Ighalo *et al.* 2021; Palanisamy *et al.* 2023). Epoxy resin (LY556) and hardener (HY951) were procured from Covai Seenu Company, located in Coimbatore, India.

Fiber Treatment

Alkali treatment was employed to improve the adhesion between the fiber and the matrix. The fibers were immersed in a 5% NaOH solution for 24 hours. Subsequent to the soaking operation, the fibers are subjected to washing and drying to remove excess alkali and moisture (Gurusamy *et al.* 2024). Alkali treatment reduces fiber hydrophilicity, improving compatibility with the hydrophobic epoxy matrix, and enhancing the mechanical performance of the composite. Figure 3 illustrates the fiber submerged in a chemical container for the purpose of chemical treatment.



Fig. 3. Fibers in chemical treatment

Composite Fabrication

The hand lay-up technique was used to fabricate the composite materials. In this process, the fibers (pat and agave) and coir dust were carefully layered in a mold, with a constant amount of epoxy resin (60%) and coir dust (10%) applied. The weight ratios of pat and agave fibers were varied to assess the impact on the composite properties (Ali *et al.* 2022). The following fiber weight ratios were used for composite fabrication. Table 1 shows sample ID and fiber varying percentages.

Table 1. Composite Formulations (Fiber percentage with Sample ID)

Sample ID	Pat fiber (P) %	Agave Fiber (A) %	Coir Dust %	Epoxy Resin %
PA1	5	25	10	60
PA2	10	20	10	60
PA3	15	15	10	60
PA4	20	10	10	60
PA5	25	5	10	60
PA6	30	0	10	60
PA7	0	30	10	60
PA8	40	0	0	60
PA9	0	40	0	60
PA10	0	0	0	100

The composite formulations (PA1–PA10) were systematically designed to evaluate the effects of fiber hybridization and coir dust filler in an epoxy matrix. In PA1–PA7, epoxy content was fixed at 60% and coir dust at 10%, while the total fiber content (30%) was varied by altering the pat and agave fiber ratios to study hybridization effects. PA1–PA5 represent different hybrid combinations of pat and agave fibers, with PA3 (15% pat and 15% agave) providing equal hybridization as shown in Fig. 4. PA6 and PA7 were single-fiber composites containing only pat or only agave fiber, respectively, along with coir dust. PA8 and PA9 contained higher fiber loading (40%) of only pat or only agave fiber without coir dust, to assess the effect of filler removal and increased reinforcement. PA10 was neat epoxy (100%) and served as the control sample for baseline comparison of mechanical, physical, and moisture absorption properties.

**Fig. 4.** PA3 Sample

Fabrication Process

Following the arrangement of the fibers and filler within the mold, the composite specimens underwent a curing process at room temperature for a duration of 24 hours, facilitating the hardening of the epoxy resin. Following this, the specimens were subjected to post-curing at 70 °C for a period of 4 h to optimize the curing process, ensuring that the epoxy matrix had reached its maximum strength, thereby improving the final mechanical properties of the composite (Balaji *et al.* 2022). The dual curing process improves the adhesion between the fibers and the matrix, resulting in the formation of strong and durable composites.

Mechanical Testing

Tensile test

The tensile test was performed in accordance with ASTM D638-14 (2022) with a universal testing machine (UTM). The test evaluates tensile strength by applying a uniaxial tensile load to the specimen until it fails. Tensile strength denotes the greatest load a material can withstand prior to failure. This test yields significant data on the material's tensile strength (Nithyanandhan *et al.* 2024). It is crucial for applications involving tensile or tensile forces, particularly in structural and load-bearing elements.

Flexural test

The flexural test was performed according to ASTM D790 (2017), employing a three-point bending configuration to evaluate the flexural strength of the composite (Gokul *et al.* 2024). A force is exerted in the center of the specimen, which is supported at both ends, resulting in bending. The flexural strength is the maximum stress that the composite can endure before failure. This test is crucial for materials utilized in applications such as beams, panels, and automobile components, where bending stresses frequently occur (Rangappa *et al.* 2022).

Hardness test

The Shore D hardness test was used to measure the surface hardness of the composites *via* ASTM D2240 (2021). This test involves using a Shore D durometer to apply a standard force to an indenter, which penetrates the surface of the material (Natrayan *et al.* 2024). The depth of indentation determines the material's hardness value. Higher values indicate greater resistance to surface deformation, which is vital for applications requiring wear resistance. Materials with high Shore D hardness are generally more durable and can withstand abrasive conditions (Stevens *et al.* 2022).

Impact test

The Izod impact test was performed following ASTM D256 (2023) standards to assess the energy absorption capacity of the composite material under impact conditions (Azad *et al.* 2022). A notched specimen undergoes impact from a pendulum hammer, and the energy required to fracture the specimen is recorded. The impact strength indicates the ability of the material to absorb energy before experiencing fracture. This test is essential for evaluating the toughness of the material and its ability to withstand unforeseen pressures or impacts, which is critical for applications in the automotive, aerospace, and construction industries (Mohammed *et al.* 2022).

Water absorption test

The water absorption test was conducted following ASTM D570 (2022) standards, with the specimens immersed in water for a duration of 48 hours. The weight increase was recorded at each time interval to assess the material's ability to absorb water (Manickaraj *et al.* 2024a). This test is critical for assessing the material's durability under humid or wet conditions. The phenomenon of high-water absorption results in swelling, a reduction in the strength of the composite, and a deterioration of mechanical properties. Consequently, this test is critical for assessing the composite's appropriateness for outdoor or marine applications (Oladele *et al.* 2020; Abhilash and Singaravelu 2022).

Thickness swelling test

Thickness swelling was determined alongside water absorption to evaluate dimensional stability. Specimen thickness was measured before and after immersion, and the percentage change was calculated. This test indicates the extent of fiber swelling and matrix softening due to moisture ingress (Alrasheedi *et al.* 2026). Lower thickness swelling values correspond to better structural stability in moisture-rich environments, making the composite suitable for marine, packaging, and outdoor applications.

Interlaminar shear strength test

Inter-laminar shear strength (ILSS) test was evaluated according to ASTM D2344 using a short-beam three-point bending method. The test measures the maximum shear stress sustained between layers of the composite before interlaminar failure occurs. ILSS is a critical indicator of fiber–matrix adhesion quality and resistance to delamination, which directly influences performance in structural, automotive, and aerospace components where shear loads are significant (Sathish *et al.* 2017).

Density

Density was determined using the Archimedes principle by measuring the mass of the specimen in air and in water. The density values were calculated to analyze material compactness, void content, and the influence of fiber and filler incorporation in the epoxy matrix (Jenish *et al.* 2021).

Scanning electron microscopic analysis

Scanning electron microscopic (SEM) analysis was conducted to examine the microstructural characteristics of the fracture surfaces. The micrographs provide insights into fiber–matrix adhesion, void formation, fiber pull-out, and failure mechanisms. Improved interfacial bonding, reduced porosity, and uniform fiber distribution observed in SEM images correlate with enhanced mechanical properties (Pandiarajan *et al.* 2025; Ravichandran *et al.* 2025). SEM thus validates the experimental findings and helps understand the structure–property relationship of the composites.

RESULTS AND DISCUSSION

Tensile Strength

The tensile strength results for the ten composite samples (PA1 to PA10) revealed a strong dependence on fiber composition, hybridization ratio, and filler presence, clearly demonstrating the effectiveness of controlled reinforcement in improving load-bearing

capacity. Sample PA1 (5% pat and 25% agave) exhibited a tensile strength of 28 MPa. The lower pat fiber fraction limits stiffness contribution, while the higher agave content may enhance ductility but not significantly improve tensile load transfer (Ramesh *et al.* 2025). Increasing the pat fiber content to 10% in PA2 improved tensile strength to 34 MPa, indicating enhanced stress transfer efficiency and improved fiber–matrix interfacial bonding. The highest tensile strength of 44 MPa was observed in PA3 (15% pat and 15% agave), confirming that equal hybridization produced an optimal synergistic effect. At this ratio, the balanced distribution of fibers likely promoted a uniform stress distribution, minimized stress concentration sites, and enhanced interfacial adhesion, resulting in superior tensile performance (Abhilash and Singaravelu 2022). However, further increasing pat fiber content led to a gradual decline in strength. PA4 (20% Pat, 10% Agave) recorded 40 MPa, and PA5 (25% pat, 5% agave) showed 36 MPa. This reduction may be attributed to reduced hybrid synergy, possible fiber agglomeration, insufficient wetting at higher fiber loadings, and localized stress concentrations (Madhu *et al.* 2019).

The performance of single-fiber systems further supports the advantage of hybridization. PA6 (30% pat) and PA7 (30% agave) exhibited tensile strengths of 33 MPa and 31 MPa, respectively, both lower than PA3, indicating that combining fibers enhanced reinforcement efficiency. In PA8 and PA9, where fiber loading increased to 40% without coir dust filler, tensile strengths were 30 and 28 MPa. The absence of particulate filler may reduce matrix continuity and interfacial support, limiting effective stress transfer. The neat epoxy (PA10) showed the lowest tensile strength of 22 MPa, confirming the significant reinforcing role of natural fibers. Figure 5 illustrates the tensile strength variation among all formulations, clearly highlighting the superior performance of the balanced hybrid composite (PA3) compared to single-fiber and non-hybrid systems.

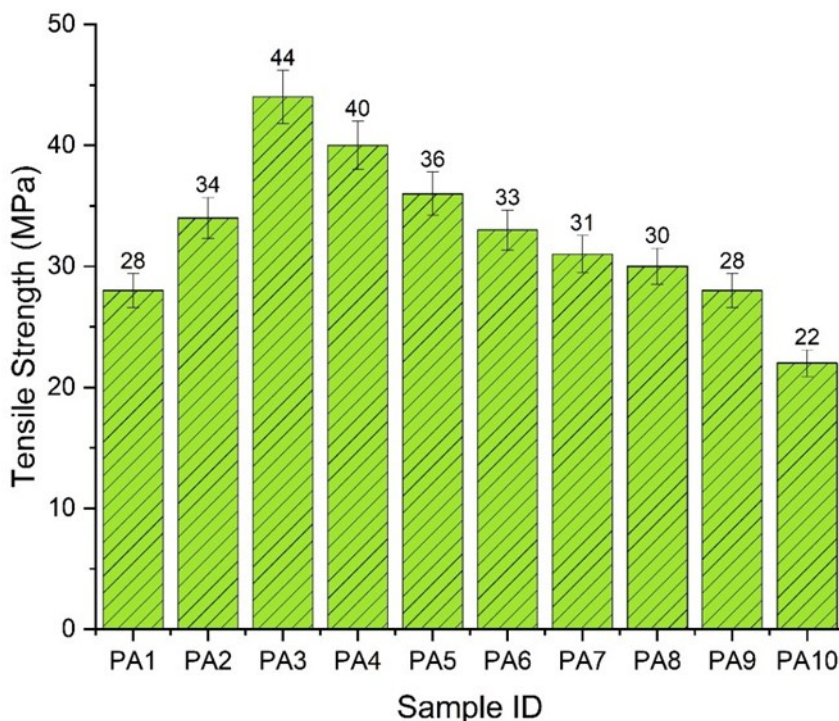


Fig. 5. Tensile test

The tensile strength of these composite materials was strongly influenced by the proportion of pat fiber, which provided stiffness and strength, while agave fiber added flexibility but may reduce tensile strength when used in excess (Oladele *et al.* 2020). The highest tensile strength was observed in PA3, where there was an optimal balance between both fibers. Samples with higher pat fiber content tended to show increased strength, but this was moderated by the amount of agave fiber, with the most favorable results occurring in PA3, which struck the best balance.

The tensile stress–strain (Fig. 6) data clearly illustrate the mechanical behavior and load-carrying capacity of the composites PA1 to PA10. All samples exhibited an initial linear increase in stress with strain, indicating elastic behavior where stress is directly proportional to strain. Among all formulations, PA3 showed the highest tensile performance, reaching a maximum stress of approximately 44 MPa at around 1.6 strain, confirming its superior strength and better load transfer capability. This indicates strong fiber–matrix bonding and effective hybrid reinforcement.

PA4 and PA5 also demonstrated high tensile strengths, reaching peak stresses of about 40 and 36 MPa respectively, but their ultimate strengths were slightly lower than PA3, suggesting that excessive dominance of one fiber slightly reduces hybrid efficiency. PA2 and PA6 exhibit moderate tensile behavior, with maximum stresses around 34 and 32 MPa, reflecting balanced but less optimized reinforcement.

PA1, PA7, PA8, and PA9 showed comparatively lower tensile strengths, indicating weaker interfacial bonding or less efficient stress transfer. The neat epoxy sample PA10 recorded the lowest tensile strength (about 22 MPa), confirming that fiber reinforcement significantly enhanced tensile performance.

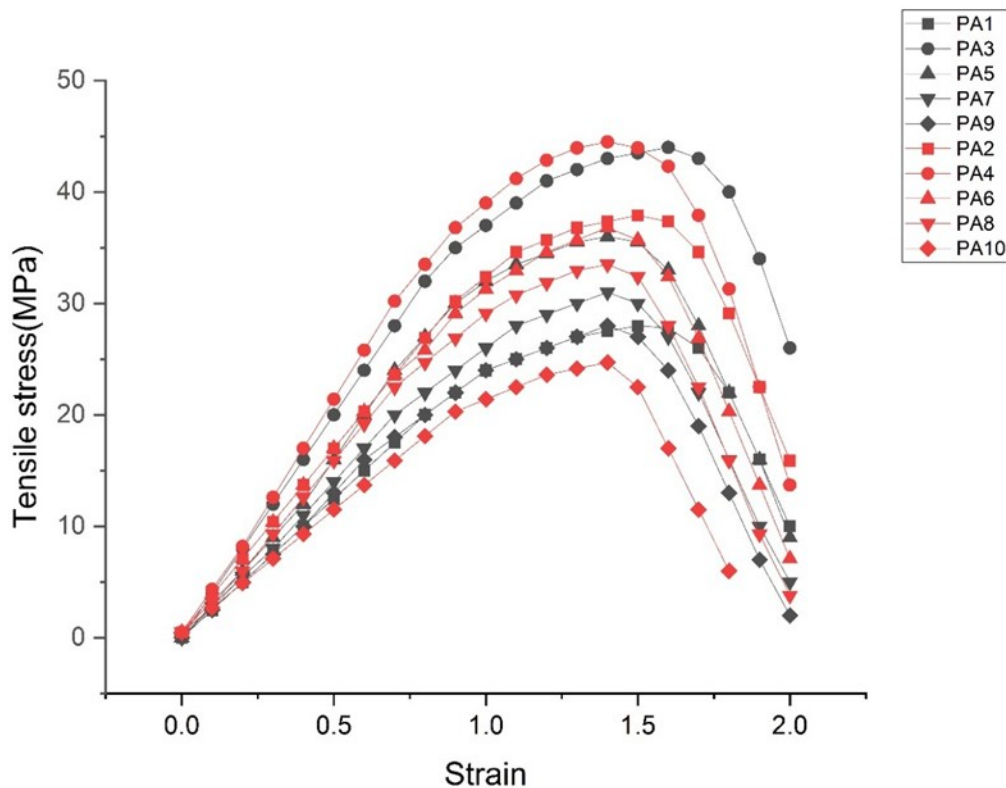


Fig. 6. Tensile stress vs. strain diagram

After reaching peak stress, all samples showed a decline in stress, representing material failure and crack propagation. PA3 maintained higher stress values for a longer strain range, indicating better toughness and ductility compared to other samples. Overall, the stress–strain behavior confirms that PA3 possesses the best tensile performance, stiffness, and structural integrity among all tested composites.

Flexural Strength

The flexural strength results for the ten composite samples (PA1 to PA10) indicated a clear influence of fiber hybridization, fiber proportion, and filler presence on bending performance. Among the hybrid composites containing coir dust (PA1–PA7), a progressive improvement in flexural strength was observed with increasing pat fiber content up to an optimal ratio. Sample PA1 (5% pat and 25% agave) exhibited the lowest flexural strength of 29 MPa, which can be attributed to the limited pat fiber reinforcement and the higher proportion of agave fiber that may contribute more to flexibility than stiffness (Athith *et al.* 2018).

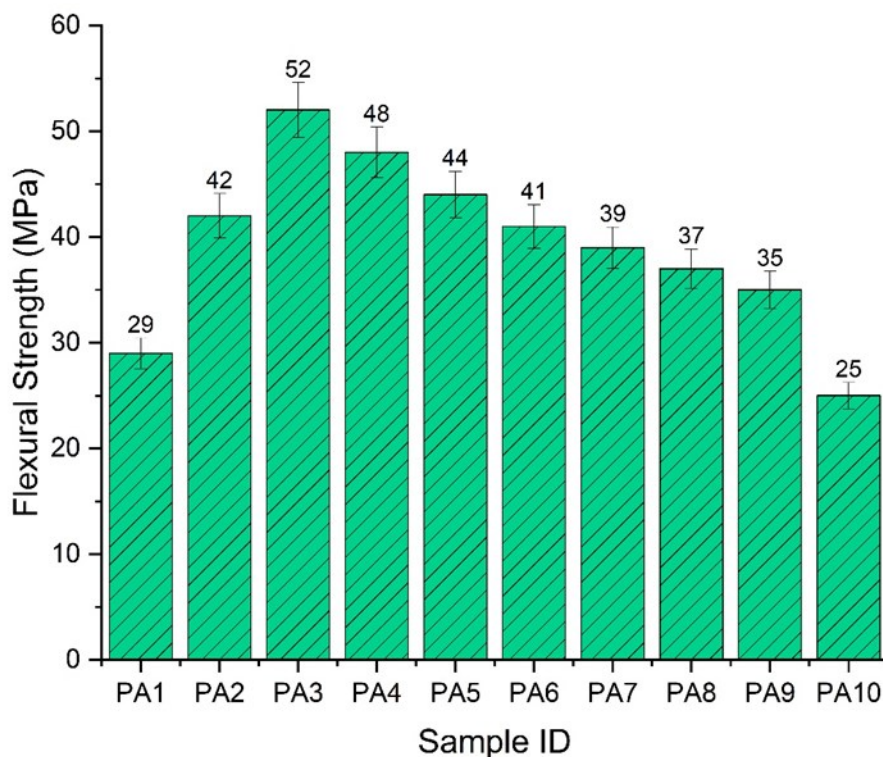


Fig. 7. Flexural test

In PA2 (10% pat and 20% agave), flexural strength increased significantly to 42 MPa, indicating improved rigidity and resistance to bending due to enhanced load transfer from matrix to fiber. The maximum flexural strength of 52 MPa was recorded for PA3 (15% pat and 15% agave), demonstrating the beneficial effect of equal hybridization. This balanced composition likely ensures uniform stress distribution under bending loads, improved interfacial bonding, and reduced stress concentration, thereby maximizing flexural performance (Agaliotis *et al.* 2022). Beyond this optimal ratio, a gradual decline was observed. PA4 (20% pat and 10% agave) recorded 48 MPa, while PA5 (25% pat and 5% agave) showed 44 MPa. Although increasing pat fiber enhanced stiffness, excessive

dominance may reduce hybrid synergy and fiber dispersion efficiency, slightly lowering performance (Palaniappan *et al.* 2024a).

The single-fiber composites PA6 (30% pat) and PA7 (30% agave) exhibited flexural strengths of 41 and 39 MPa, respectively, confirming that hybrid reinforcement provided superior bending resistance compared to individual fiber systems. In PA8 and PA9, with 40% single-fiber loading and no coir dust, flexural strengths decreased to 37 and 35 MPa, suggesting reduced matrix continuity and filler support. The neat epoxy (PA10) showed the lowest value of 25 MPa, confirming the reinforcing effect of fibers. Figure 7 presents the flexural test results.

The flexural strength of these materials is largely influenced by the proportion of pat fiber, with higher pat fiber content leading to better resistance to bending and deformation (Vijay and Singaravelu 2016). PA3 exhibited the highest flexural strength due to an optimal balance between pat fiber and agave fiber, while PA1, with minimal pat fiber, showed the lowest flexural strength.

The flexural stress–strain results (Fig. 8) clearly demonstrate the bending performance and load-bearing capacity of the composites PA1 to PA10. Initially, all samples showed a steady linear increase in flexural stress with increasing strain, indicating elastic deformation under bending load. Among all formulations, PA3 exhibited the highest flexural strength, reaching a maximum of approximately 52 MPa at around 2.1 strain. It also sustained load over a wider strain range before failure, confirming superior stiffness, better fiber–matrix adhesion, and enhanced resistance to crack propagation under bending.

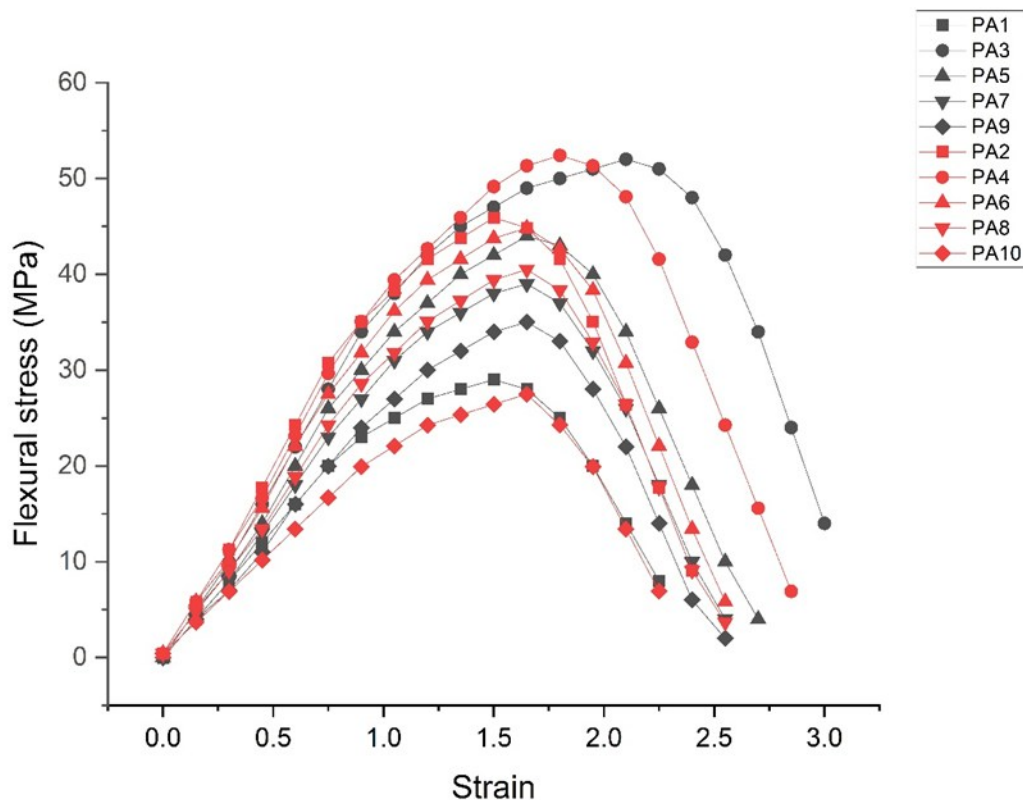


Fig. 8. Flexural stress vs. strain diagram

PA4 and PA5 also showed strong flexural behavior, achieving peak stresses of about 48 and 44 MPa respectively. However, their failure occurred earlier than PA3, suggesting slightly lower ductility and hybrid efficiency. PA2 and PA6 demonstrated moderate performance, with maximum stresses of approximately 42 and 41 MPa, indicating improved reinforcement but not as optimized as PA3.

PA1, PA7, PA8, and PA9 exhibited comparatively lower peak stresses and earlier failure, reflecting weaker interfacial bonding, possible void formation, or less effective stress transfer between fiber and matrix. The neat epoxy sample PA10 showed the lowest flexural strength (about 25 MPa) and failed abruptly, confirming its brittle nature and the importance of fiber reinforcement in improving bending resistance.

After reaching peak stress, most samples showed a gradual decline, representing crack initiation and propagation. Notably, PA3 maintained higher residual stress for a longer strain range, indicating improved toughness and structural stability. Overall, the flexural behavior confirmed that PA3 had the best bending strength, stiffness, and durability among all tested composites.

Impact Strength

The impact strength results for the ten composite samples (PA1 to PA10) illustrate the influence of fiber hybridization, composition balance, and filler presence on energy absorption capacity under sudden loading. Among the hybrid composites containing coir dust (PA1 to PA7), impact strength generally increased with increasing Pat fiber content up to an optimal hybrid ratio. Sample PA1 (5% pat and 25% agave) exhibited the lowest impact strength among the hybrids at 0.28 J, which may be attributed to insufficient reinforcement from the lower Pat fiber content, despite the flexibility contributed by agave fiber (Sumesh *et al.* 2021; Kumar *et al.* 2024).

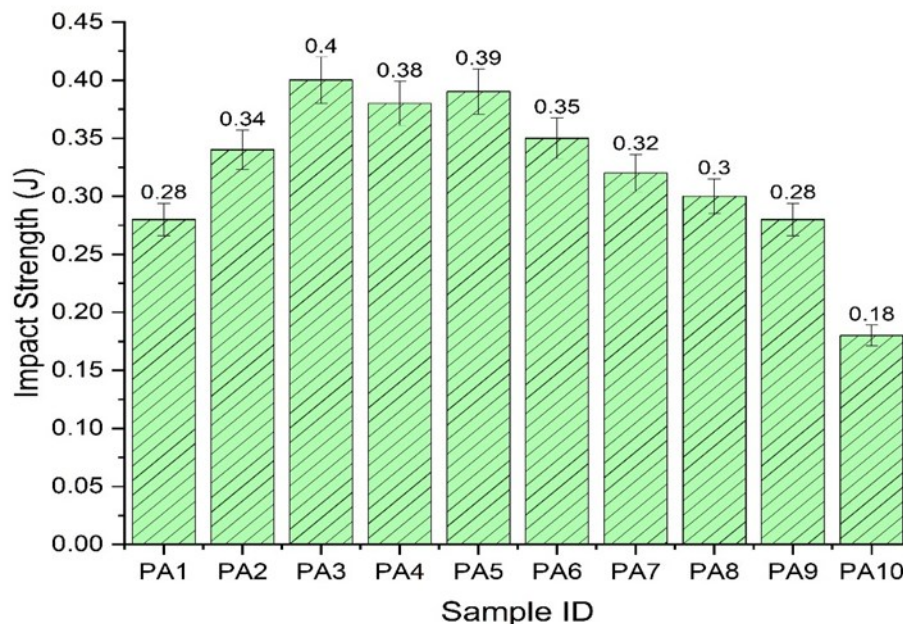


Fig. 9. Impact strength

In PA2 (10% pat and 20% agave), impact strength increased to 0.34 J, indicating improved resistance to crack initiation and propagation due to enhanced fiber–matrix interaction. The highest impact strength of 0.40 J was recorded for PA3 (15% pat and 15% agave), demonstrating the advantage of balanced hybridization (Aruchamy *et al.* 2025). At this composition, the combination of stiffness from pat fiber and flexibility from agave fiber likely promotes effective energy dissipation mechanisms such as fiber pull-out, crack deflection, and interfacial debonding.

PA4 (20% pat and 10% agave) showed a slightly lower value of 0.38 J (Karupppiah *et al.* 2020), suggesting that excessive stiffness may reduce impact energy absorption efficiency. Interestingly, PA5 (25% pat and 5% agave) recorded 0.39 J, slightly higher than PA4, indicating that moderate increases in Pat fiber still contribute to impact resistance, though not surpassing the balanced PA3 system (Prasad *et al.* 2023).

The single-fiber composites PA6 (30% pat) and PA7 (30% agave) exhibited 0.35 J and 0.32 J, respectively, confirming that hybridization enhanced impact performance compared to individual fiber systems. In PA8 and PA9, with 40% single-fiber loading and no coir dust, impact strength decreased to 0.30 and 0.28 J, likely due to reduced matrix continuity and limited crack-bridging mechanisms. The neat epoxy sample (PA10) showed the lowest impact strength of 0.18 J, highlighting the significant role of natural fiber reinforcement in improving toughness. Figure 9 shows the impact test results.

Overall, the impact strength of the samples seemed to correlate with the balance between pat fiber and agave fiber, with a higher proportion of pat fiber generally increasing strength but possibly reducing the material's ability to absorb impact energy. PA3, with its balanced composition of 15% pat and 15% agave fiber, performed the best in terms of impact strength, providing a good compromise between flexibility and stiffness.

Hardness

The hardness results for the ten composite samples (PA1 to PA10) indicated a strong dependence on fiber composition, hybridization ratio, and reinforcement distribution within the epoxy matrix. Among the hybrid composites containing coir dust (PA1 to PA7), hardness generally increased with increasing pat fiber content up to an optimal balance. Sample PA1 (5% pat and 25% agave) exhibited the lowest hardness among the hybrid systems at 72 SD, which may be attributed to the higher proportion of agave fiber that contributes more flexibility than surface rigidity.

In PA2 (10% pat and 20% agave), hardness increased to 78 SD, reflecting improved resistance to indentation due to enhanced stiffness from the higher pat fiber content. The maximum hardness value of 84 SD was observed in PA3 (15% pat and 15% agave), demonstrating that equal hybridization results in superior surface resistance. The balanced distribution of fibers likely improves load sharing at the microstructural level and enhances matrix constraint, thereby increasing resistance to localized deformation (Hulle *et al.* 2015; Ramesh *et al.* 2023).

In PA4 (20% pat and 10% agave), hardness slightly decreased to 82 SD. Although Pat fiber content increased, the reduced agave proportion may affect the internal stress distribution and hybrid synergy. PA5 (25% pat and 5% agave) recorded 79 SD, indicating that excessive dominance of a single fiber does not further improve hardness and may slightly reduce overall structural balance (Yawas *et al.* 2016; Nayak *et al.* 2022).

The single-fiber systems PA6 (30% pat) and PA7 (30% agave) exhibited hardness values of 80 SD and 77 SD, respectively, confirming that hybrid composites performed better than individual fiber systems. In PA8 and PA9, with 40% single-fiber loading and

no coir dust, hardness decreased to 75 and 73 SD, which was likely due to reduced filler reinforcement and matrix continuity. The neat epoxy sample (PA10) showed the lowest hardness of 70 SD, highlighting the reinforcing contribution of natural fibers. Figure 10 shows the hardness test results.

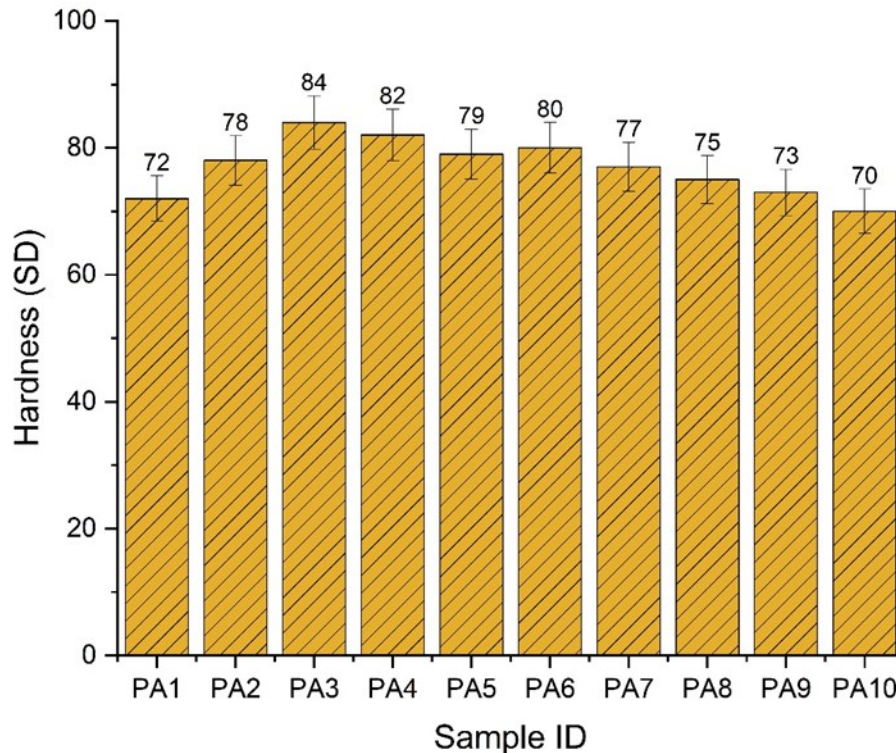


Fig. 10. Hardness test

Interlaminar Shear Strength

Interlaminar shear strength (ILSS) reflects the composite's resistance to failure between adjacent layers under transverse shear loading and is primarily governed by fiber–matrix adhesion, fiber dispersion, and matrix continuity. In the present study, ILSS values ranged from 4 to 9 MPa across PA1 to PA10, clearly indicating the influence of hybrid fiber proportion and filler presence (Sathish *et al.* 2017).

Among all formulations, PA3 exhibited the highest ILSS of 9 MPa, confirming that the balanced hybrid configuration (15% pat and 15% agave with 10% coir dust) promoted superior interfacial bonding and efficient stress transfer through the laminate thickness. The optimized fiber ratio likely enhanced packing density and uniform resin wetting, minimizing microvoid formation. Chemically treated fibers further improved compatibility with the epoxy matrix, strengthening mechanical interlocking and reducing interlaminar debonding under shear stresses (Aruchamy *et al.* 2025).

In contrast, PA1 showed a lower ILSS of 5 MPa, indicating weaker interface quality and possible non-uniform fiber dispersion. The disproportionate fiber ratio may cause localized agglomeration and resin-rich zones, limiting effective shear load transfer. Moisture sensitivity at the interface can further weaken adhesion and reduce shear resistance (Manickaraj *et al.* 2025).

Intermediate hybrid samples PA2 (6.8 MPa), PA4 (8.2 MPa), and PA5 (7.5 MPa) demonstrated gradual improvement but remained inferior to PA3, suggesting moderate interface efficiency. Single-fiber systems PA6 (6.5 MPa) and PA7 (6.2 MPa), along with

high-fiber formulations without filler PA8 (6 MPa) and PA9 (5.6 MPa), exhibited comparatively lower ILSS due to reduced hybrid synergy and filler-assisted bonding. The neat epoxy PA10 showed the lowest value (4 MPa), confirming the critical role of fiber reinforcement in enhancing interlaminar integrity. Overall, PA3 demonstrated the most stable and durable laminate structure. Figure 11 shows the ILSS results.

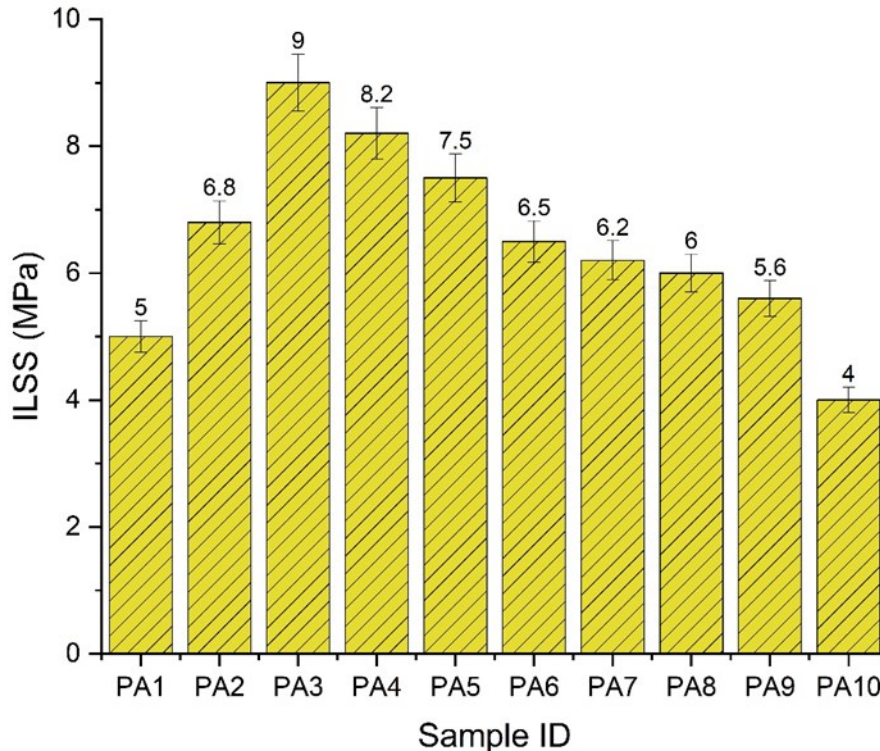


Fig. 11. Interlaminar shear strength

Water Absorption

The water absorption results for the ten composite samples (PA1 to PA10) demonstrated a strong influence of fiber composition, hybridization balance, and filler presence on moisture uptake behavior. Among the hybrid composites containing coir dust (PA1 to PA7), water absorption ranged between 10% and 16%, indicating differences in fiber–matrix compatibility and void content. Sample PA1 (5% pat and 25% agave) exhibited 16% water absorption, which can be attributed to the higher agave fiber content, as agave fibers are comparatively more hydrophilic and contain higher cellulose content, promoting moisture diffusion (Sathish *et al.* 2017; Sumesh *et al.* 2024).

In PA2 (10% pat and 20% agave), water absorption decreased to 14%, which was likely due to the increased pat fiber proportion, which may reduce the number of hydrophilic sites and improve matrix bonding. The lowest water absorption of 10% was observed in PA3 (15% pat and 15% agave), indicating that balanced hybridization enhanced dimensional stability and reduced capillary pathways for water ingress (Venkateshwaran *et al.* 2011; Prasad *et al.* 2023; Mahalingam 2024). Improved fiber dispersion and better interfacial adhesion in PA3 likely minimized microvoids and restricted moisture penetration.

In PA4 (20% pat and 10% agave), water absorption slightly increased to 13%, suggesting that excessive dominance of one fiber may affect uniform stress distribution

and matrix continuity. PA5 (25% pat and 5% agave) showed 15% absorption, indicating that higher pat content alone did not guarantee improved moisture resistance.

The single-fiber systems PA6 (30% pat) and PA7 (30% agave) recorded 15% and 16% absorption, respectively, confirming the benefit of hybridization. Higher fiber loading without coir dust in PA8 (17%) and PA9 (18%) resulted in greater moisture uptake due to increased fiber exposure and reduced matrix continuity. The neat epoxy PA10 exhibited minimal absorption (1.2%), confirming the hydrophobic nature of the matrix. Figure 12 shows the water absorption test results.

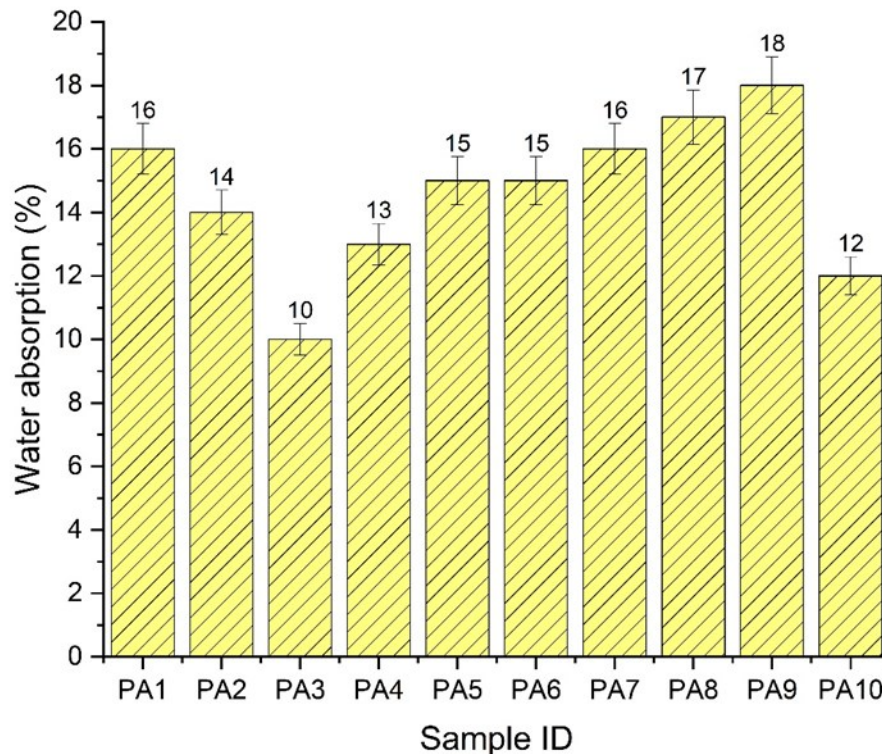


Fig. 12. Water absorption test

The water absorption tended to decrease with the increase in pat fiber content, as pat fiber is less water-absorbent than agave fiber. The samples with higher agave fiber (PA1, PA5) showed higher water absorption, while PA3, with a balanced fiber composition, demonstrated the lowest water absorption.

Thickness Swelling

Thickness swelling is a critical parameter for evaluating the dimensional stability of natural fiber-reinforced composites under humid or immersed conditions. In the present study, swelling values ranged from 0.5% to 4%, closely following the water absorption trend and confirming the influence of fiber hydrophilicity, fiber-matrix adhesion, and void distribution (Chiang *et al.* 2014; Ahmad *et al.* 2023).

Among the hybrid composites containing coir dust (PA1–PA7), PA3 exhibited the lowest thickness swelling of 2.3%, indicating superior dimensional stability. The balanced hybrid ratio (15% pat and 15% agave) likely ensured uniform fiber dispersion, improved packing density, and effective resin impregnation, thereby minimizing microvoids and restricting capillary pathways for moisture ingress. Strong interfacial bonding due to chemical treatment enhances matrix constraint over fiber expansion, limiting swelling

during water exposure (Karuppusamy *et al.* 2025).

Conversely, PA1 recorded higher swelling of 3.6%, suggesting reduced dimensional stability. The disproportionate fiber ratio may promote fiber clustering and incomplete resin wetting, forming microchannels that facilitate moisture penetration and fiber expansion. Intermediate values observed in PA2 (3.2%), PA4 (2.9%), and PA5 (3.4%) indicate moderate improvements in hybrid interaction and matrix continuity, though not as effective as PA3.

Single-fiber systems PA6 (3.3%) and PA7 (3.5%) showed comparatively higher swelling, confirming the advantage of hybridization. Higher fiber loading without filler in PA8 (3.8%) and PA9 (4%) resulted in maximum swelling due to increased fiber exposure and reduced matrix confinement. The neat epoxy sample PA10 exhibited minimal swelling (0.5%), reflecting its hydrophobic nature. Overall, PA3 demonstrated optimal resistance to moisture-induced dimensional change. Figure 13 shows the thickness swelling.

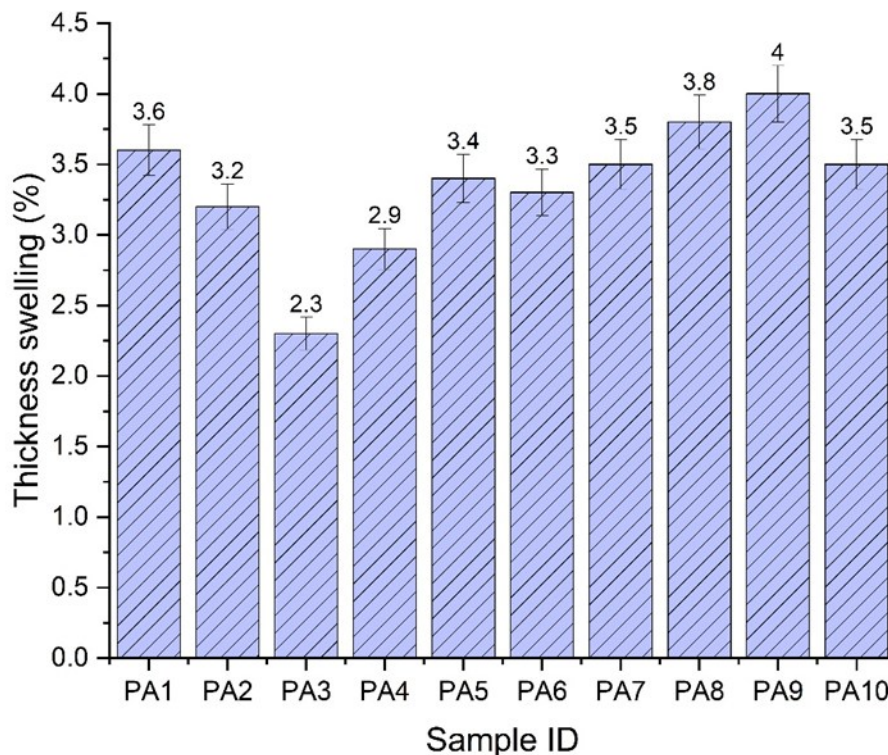


Fig. 13. Thickness swelling

Density

The density results of the hybrid composites (PA1 to PA9) ranged from 1.27 to 1.36 g/cm³, indicating that fiber proportion and filler distribution significantly influenced the compactness and internal structure of the laminates. Density is an important physical parameter because it reflects the degree of fiber packing, matrix infiltration, and void content within the composite. Lower density values often indicate higher void content or insufficient resin wetting, whereas higher values suggest better consolidation and reduced porosity. Among the samples, PA1 recorded the lowest density of 1.27 g/cm³. This relatively lower value may be attributed to uneven fiber dispersion and possible microvoid formation due to higher agave fiber content, which can hinder effective matrix penetration. PA2 showed a slight increase to 1.29 g/cm³, indicating improved packing and reduced void content as the pat fiber proportion increased.

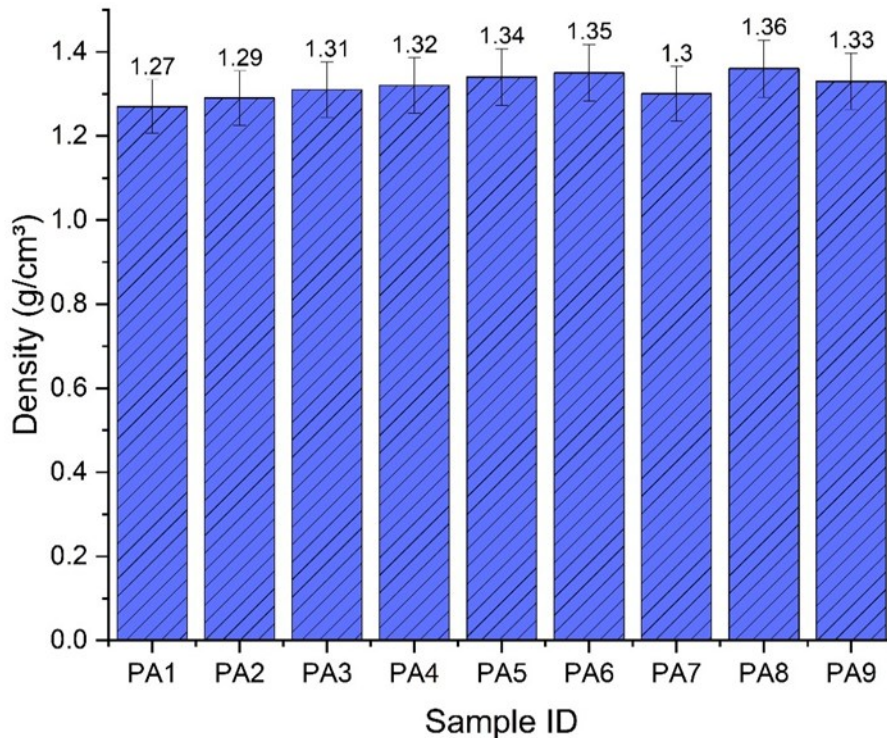


Fig. 14. Density

PA3 exhibited a density of 1.31 g/cm³, suggesting better fiber–matrix interaction and more uniform structural integrity due to its balanced hybrid composition. Further increasing the Pat fiber content in PA4 and PA5 resulted in densities of 1.32 and 1.34 g/cm³, respectively. These values reflect improved compaction and enhanced matrix continuity, which contributed to better mechanical performance. PA6 showed a density of 1.35 g/cm³, indicating strong consolidation when pat fiber dominated the reinforcement system. PA7, containing higher agave fiber content, recorded 1.30 g/cm³, slightly lower than PA6, possibly due to differences in fiber morphology and moisture affinity. The highest density was observed in PA8 (1.36 g/cm³), which may be attributed to higher fiber loading and improved laminate compression during fabrication. PA9 exhibited 1.33 g/cm³, slightly lower than PA8, likely due to differences in fiber distribution and internal porosity. Overall, the gradual increase in density from PA1 to PA8 suggests improved packing efficiency and reduced void formation with optimized fiber content, which positively influenced the mechanical and structural stability of the composites. Figure 14 shows the density results.

Scanning Electron Microscopic Analysis

The SEM micrographs provide clear evidence of the fracture morphology, fiber–matrix interaction, and failure mechanisms governing the mechanical behavior of the hybrid composites. Distinct differences in interfacial bonding and structural integrity were observed among the samples, closely aligning with the mechanical, physical, and durability test results. In PA3, the fracture surface exhibited excellent fiber–matrix adhesion, with well-embedded fibers, minimal interfacial gaps, and a compact resin-rich structure. The absence of significant voids and limited fiber pull-out indicated efficient stress transfer across the interface, which explains its superior tensile, flexural, hardness, and ILSS

performance, along with its lowest water absorption (10%) and thickness swelling (2.3%) (Palanisamy *et al.* 2022b; Kuriakose Mani *et al.* 2025; Nanthakumar *et al.* 2025). The uniform dispersion of pat and agave fibers confirmed optimal hybrid packing and effective resin wetting.

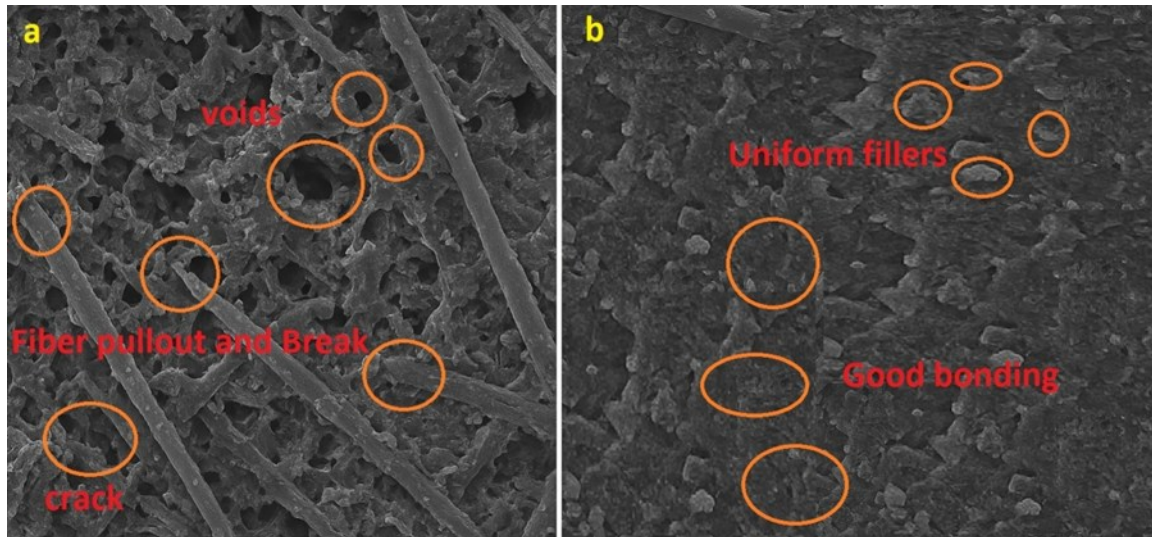


Fig. 15. a: PA1 (Pat 5%, Agave 25%, coir 10%); and b: PA3 (Pat 15%, Agave 15%, coir 10%)

In contrast, PA1 (Fig. 15a) displayed numerous voids, microcracks, and extensive fiber pull-out regions, reflecting weak interfacial bonding and insufficient matrix penetration (Palanisamy *et al.* 2022b; Palaniappan *et al.* 2024b). Visible fiber debonding and interfacial gaps indicate poor adhesion, which correlated with its lower mechanical strength, lower ILSS (5 MPa), higher water absorption (16%), and higher thickness swelling (3.6%). Fiber clustering and resin-starved zones further contributed to uneven stress distribution and premature fracture.

The intermediate samples PA2, PA4, and PA5 showed moderate morphological features, with improved adhesion compared to PA1 but still containing scattered microvoids and localized debonding. These imperfections explain their moderate mechanical and moisture-resistance properties. PA6 and PA7 exhibited more pronounced fiber pull-out due to single-fiber dominance, while PA8 and PA9 revealed increased porosity associated with higher fiber loading. The neat epoxy sample PA10 showed a smooth, brittle fracture surface without fiber-related defects. Overall, the SEM observations confirm that optimized hybridization and strong interfacial bonding, as seen in PA3 (Fig. 15b), were critical for enhanced composite performance.

CONCLUSIONS

The comprehensive evaluation of tensile strength, flexural strength, impact strength, interlaminar shear strength (ILSS), hardness, water absorption, thickness swelling, and density clearly demonstrates that composite performance was highly dependent on fiber composition and hybridization balance. Among all formulations (PA1 to PA10), PA3 consistently exhibited superior overall properties, confirming the effectiveness of an optimized hybrid configuration.

PA3 achieved the highest tensile strength (44 MPa), flexural strength (52 MPa),

impact strength (0.4 J), ILSS (9 MPa), and hardness (84 SD). It also recorded the lowest water absorption (10%) and thickness swelling (2.3%) among the hybrid composites, along with a moderate density of 1.31 g/cm³, indicating good consolidation with minimal void content. These results confirm that a balanced proportion of pat and agave fibers promotes efficient stress transfer, improved packing density, and enhanced fiber–matrix interfacial bonding.

Although PA4 and PA5 showed comparatively high strength and hardness due to increased pat fiber content, their performance was slightly inferior to PA3, suggesting that excessive dominance of one fiber reduces hybrid synergy. Samples with higher agave content such as PA1 exhibited lower mechanical properties (28 MPa tensile, 29 MPa flexural) and higher water absorption (16%) and swelling (3.6%), indicating weaker interfacial adhesion and greater moisture susceptibility.

Single-fiber dominant systems (PA6 and PA7) and higher fiber loading samples (PA8 and PA9) showed moderate strength but increased water absorption and swelling, likely due to fiber clustering and microvoid formation. The neat epoxy sample PA10 demonstrated the lowest mechanical properties (22 MPa tensile, 25 MPa flexural, 4 MPa ILSS) but exhibited minimal water absorption (1.2%) and swelling (0.5%), confirming that reinforcement is essential for mechanical enhancement, while the matrix alone offers better moisture resistance.

Scanning electron microscopy (SEM) analysis strongly supports these findings. PA3 displayed a compact and uniform fracture surface with minimal fiber pull-out, fewer voids, and strong fiber–matrix adhesion, confirming efficient load transfer and structural integrity. In contrast, PA1, PA8, and PA9 showed noticeable fiber debonding, microcracks, voids, and resin-starved regions, explaining their lower strength and higher moisture uptake. PA4 and PA5 exhibited intermediate morphology with moderate adhesion and occasional microvoids, correlating with their balanced but slightly reduced performance compared to PA3. Overall, the study confirms that optimized hybridization, uniform fiber dispersion, and strong interfacial bonding are critical for maximizing mechanical strength and durability. Among all samples, PA3 represented the optimal formulation, providing the best combination of strength, toughness, interlaminar integrity, dimensional stability, and structural compactness.

FUNDING

This work was supported and funded by the Deanship of Scientific Research at Imam Mohammad Ibn Saud Islamic University (IMSIU) (grant number IMSIU-DDRSP2602).

Data Availability Statement

Data are available on request from the authors.

Declaration of Conflicting Interests

The authors declared no potential conflicts of interest with respect to the research, authorship, and/or publication of this article.

REFERENCES CITED

- Abhilash, S. S., and Singaravelu, D. L. (2022). "A comparative study of mechanical, morphological and vibration damping characteristics of wood fiber reinforced LLDPE processed by rotational moulding," *Materials Today: Proceedings* 59, 510–515. <https://doi.org/10.1016/j.matpr.2021.11.559>
- Agaliotis, E. M., Ake-Concha, B. D., May-Pat, A., Morales-Arias, J. P., Bernal, C., Valadez-Gonzalez, A., Herrera-Franco, P. J., Proust, G., Koh-Dzul, J. F., and Carrillo, J. G. (2022). "Tensile behavior of 3D printed polylactic acid (PLA) based composites reinforced with natural fiber," *Polymers* 14(19), article 3976. <https://doi.org/10.3390/polym14193976>
- Ahmad, M. N., Ishak, M. R., Mohammad Taha, M., Mustapha, F., Leman, Z., and Irianto. (2023). "Mechanical, thermal and physical characteristics of oil palm (*Elaeis Guineensis*) fiber reinforced thermoplastic composites for FDM – Type 3D printer," *Polymer Testing* 120, article 107972. <https://doi.org/10.1016/j.polymertesting.2023.107972>
- Ali, M., Alabdulkarem, A., Nuhait, A., Al-Salem, K., Iannace, G., and Almuzaifer, R. (2022). "Characteristics of agro waste fibers as new thermal insulation and sound absorbing materials: hybrid of date palm tree leaves and wheat straw fibers," *Journal of Natural Fibers* 19(13), 6576-6594. <https://doi.org/10.1080/15440478.2021.1929647>
- Alrasheedi, N. H., Sivasubramanian, P., Karuppusamy, M., Haldar, B., and Durairaj, T. K. (2026). "Hybrid bio-composites reinforced with kenaf and snake grass fibers and neem gum: synergistic effects and role of fiber aspect ratio," *BioResources* 21(1), 459-481. <https://doi.org/10.15376/biores.21.1.459-481>
- Aruchamy, K., Karuppusamy, M., Krishnakumar, S., Palanisamy, S., Jayamani, M., Sureshkumar, K., Ali, S. K., and Al-Farraj, S. A. (2025). "Enhancement of mechanical properties of hybrid polymer composites using palmyra palm and coconut sheath fibers: The role of tamarind shell powder," *BioResources* 20(1), 698-724. <https://doi.org/10.15376/biores.20.1.698-724>
- ASTM D2240-15 (2021). "Standard test method for rubber property—Durometer hardness," ASTM International, West Conshohocken, PA, USA.
- ASTM D6110-18 (2010). "Standard test method for determining the Charpy impact resistance of notched specimens of plastics," International Organization for Standardization: Geneva, Switzerland, 2010.
- ASTM D570-22 (2022). "Standard test method for water absorption of plastics," ASTM International, West Conshohocken, PA, USA.
- ASTM D695 – 15 (2015), "Standard test method for compressive properties of rigid plastics," American Society for Testing and Materials, 2015.
- ASTM D638-14 (2022). "Standard test method for tensile properties of plastics," ASTM International, West Conshohocken, PA, USA.
- ASTM D790-17 (2017). "Standard test methods for flexural properties of unreinforced and reinforced plastics and electrical insulating materials," ASTM International, West Conshohocken, PA, USA.
- ASTM D792-13 (2013). "Standard Test methods for density and specific gravity (relative density) of plastics by displacement," in: *Annual Book of ASTM*, 2013.
- Athith, D., Sanjay, M. R., Yashas Gowda, T. G., Madhu, P., Arpitha, G. R., Yogesha, B., and Omri, M. A. (2018). "Effect of tungsten carbide on mechanical and tribological

- properties of jute/sisal/E-glass fabrics reinforced natural rubber/epoxy composites,” *Journal of Industrial Textiles* 48(4), 713-737.
<https://doi.org/10.1177/1528083717740765>
- Ayrilmis, N., Kanat, G., Yildiz Avsar, E., Palanisamy, S., and Ashori, A. (2024). “Utilizing waste manhole covers and fibreboard as reinforcing fillers for thermoplastic composites,” *Journal of Reinforced Plastics and Composites* 07316844241238507. <https://doi.org/10.1177/07316844241238507>
- Azad, M. M., Ejaz, M., Afaq, S. K., and Song, J. (2022). “Static mechanical properties of bio-fiber-based polymer composites,” in: *Advances in Bio-Based Fiber* Ch 5, 97-139. <https://doi.org/10.1016/B978-0-12-824543-9.00034-7>
- Badyankal, P. V, Manjunatha, T. S., Vaggar, G. B., and Praveen, K. C. (2021). “Compression and water absorption behaviour of banana and sisal hybrid fiber polymer composites,” *Materials Today: Proceedings* 35, 383-386. <https://doi.org/10.1016/j.matpr.2020.02.695>
- Balaji, A., Kannan, S., Purushothaman, R., Mohanakannan, S., Maideen, A. H., Swaminathan, J., Karthikeyan, B., and Premkumar, P. (2022). “Banana fiber and particle-reinforced epoxy biocomposites: mechanical, water absorption, and thermal properties investigation,” *Biomass Conversion and Biorefinery* 14, 1-11. <https://doi.org/10.1007/s13399-022-02829-y>
- Bhuvaneswari, V., Devarajan, B., Arulmurugan, B., Mahendran, R., Rajkumar, S., Sharma, S., Mausam, K., Li, C., and Eldin, E. T. (2022). “A critical review on hygrothermal and sound absorption behavior of natural-fiber-reinforced polymer composites,” *Polymers* 14(21), article 4727. <https://doi.org/10.3390/polym14214727>
- Del Campo, A. S. M., Robledo-Ortíz, J. R., Arellano, M., Jasso-Gastinel, C. F., Silva-Jara, J. M., López-Naranjo, E. J., and Pérez-Fonseca, A. A. (2020). “Glycidyl methacrylate-compatible poly (lactic acid)/nanoclay/agave fiber hybrid biocomposites: Effect on the physical and mechanical properties,” *Revista Mexicana de Ingeniería Química* 19(1), 455-469. <https://doi.org/10.24275/rmiq/Mat627>
- Chiang, T. C., Osman, M. S., and Hamdan, S. (2014). “Water absorption and thickness swelling behavior of sago particles urea formaldehyde particleboard,” *International Journal of Science and Research (IJSR)* 3(12), 1375-1379.
- Chithra, N. V, Karuppasamy, R., Manickaraj, K., and Ramakrishnan, T. (2024). “Effect of reinforcement addition on mechanical behavior of Al MMC-A critical review,” *J. Environ. Nanotechnol* 13(2), 65-79. <https://doi.org/10.13074/jent.2024.06.242632>
- Cisneros-López, E. O., González-López, M. E., Pérez-Fonseca, A. A., González-Núñez, R., Rodrigue, D., and Robledo-Ortíz, J. R. (2017). “Effect of fiber content and surface treatment on the mechanical properties of natural fiber composites produced by rotomolding,” *Composite Interfaces* 24(1), 35-53. <https://doi.org/10.1080/09276440.2016.118455>
- Dharmaratne, P. D., Galabada, H., Jayasinghe, R., Nilmini, R., and Halwatura, R. U. (2021). “Characterization of physical, chemical and mechanical properties of Sri Lankan coir fibers,” *Journal of Ecological Engineering* 22(6), 55-65.
- Dugvekar, M., and Dixit, S. (2022). “Chemical treatments for modification of the surface morphology of coir fiber: A review,” *Journal of Natural Fibers* 19(15), 11940-11961. <https://doi.org/10.1080/15440478.2022.2048938>
- Gokul, S., Ramakrishnan, T., Manickaraj, K., Devadharshan, P., Mathew, M. K., and Prabhu, T. V. (2024). “Analyzing challenges and prospects for sustainable development with green energy: A comprehensive review,” in: *AIP Conference*

- Proceedings* 3221, article 020043. <https://doi.org/10.1063/5.0235884>
- Goutham, E. R. S., Hussain, S. S., Muthukumar, C., Krishnasamy, S., Kumar, T. S. M., Santulli, C., Palanisamy, S., Parameswaranpillai, J., and Jesuarockiam, N. (2023). "Drilling parameters and post-drilling residual tensile properties of natural-fiber-reinforced composites: A review," *Journal of Composites Science* 7(4), article 136. <https://doi.org/10.3390/jcs7040136>
- Govindarajan, P. R., Antony, J. A., Palanisamy, S., Ayrilmis, N., Khan, T., Junaedi, H., and Sebaey, T. A. (2024). "Advances in manufacturing of carbon-based molecular nanomaterials based on rice husk/hull waste," *BioResources* 19(4), 9834-9852. <https://doi.org/10.15376/biores.19.4.govindarajan>
- Gunti, R., Ratna Prasad, A.V., and Gupta, A. V. S. S. K. S. (2018). "Mechanical and degradation properties of natural fiber-reinforced PLA composites: Jute, sisal, and elephant grass," *Polymer Composites* 39(4), 1125-1136. <https://doi.org/10.1002/pc.24041>
- Gupta, N., and Ramkumar, P. L. (2021). "Effect of coir content on mechanical and thermal properties of LLDPE/coir blend processed by rotational molding," *Sādhanā* 46(1), article 40. <https://doi.org/10.1007/s12046-021-01566-8>
- Gurusamy, M., Soundararajan, S., Karuppusamy, M., and Ramasamy, K. (2024). "Exploring the mechanical impact of fine powder integration from ironwood sawdust and COCO dust particles in epoxy composites," *Matéria (Rio de Janeiro)*, 29, article e20240216. <https://doi.org/10.1590/1517-7076-RMAT-2024-0216>
- Hulle, A., Kadole, P., and Katkar, P. (2015). "Agave Americana leaf fibers," *Fibers* 3(1), 64-75. <https://doi.org/10.3390/fib3010064>
- Ibrahim, I. D., Jamiru, T., Sadiku, E. R., Kupolati, W. K., Agwuncha, S. C., and Ekundayo, G. (2016). "Mechanical properties of sisal fibre-reinforced polymer composites: A review," *Composite Interfaces* 23(1), 15-36. <https://doi.org/10.1080/09276440.2016.1087247>
- Ighalo, J. O., Adeniyi, A. G., Owolabi, O. O., and Abdulkareem, S. A. (2021). "Moisture absorption, thermal and microstructural properties of polymer composites developed from rice husk and polystyrene wastes," *International Journal of Sustainable Engineering* 14(5), 1049-1058. <https://doi.org/10.1080/19397038.2021.1892234>
- Jenish, I., Felix Sahayaraj, A., Appadurai, M., Fantin Irudaya Raj, E., Suresh, P., Raja, T., Salmen, S.H., Alfarraj, S. and Manikandan, V. (2021). "Fabrication and experimental analysis of treated snake grass fiber reinforced with polyester composite," *Advances in Materials Science and Engineering* 2021(1), article 6078155. <https://doi.org/10.1155/2021/6078155>
- Kar, A., Saikia, D., Palanisamy, S., and Pandiarajan, N. (2024). "Calamus tenuis fiber reinforced epoxy composites: Effect of fiber loading on the tensile, structural, crystalline, thermal and morphological characteristics," *Journal of Polymer Research* 31(11), 1-16. <https://doi.org/10.1007/s10965-024-04162-6>
- Karuppiyah, G., Kuttalam, K. C., and Palaniappan, M. (2020). "Multiobjective optimization of fabrication parameters of jute fiber / polyester composites with egg shell powder and nanoclay filler," *Molecules* 25(23), article 5579. <https://doi.org/10.3390/molecules25235579>
- Karuppusamy, M., Kalidas, S., Palanisamy, S., Nataraj, K., Nandagopal, R. K., Natarajan, R., Samraj, A., Ayrilmis, N., Sahu, S. K., and Giri, J. (2025). "Real-time monitoring in polymer composites: internet of things integration for enhanced performance and sustainability—A review," *BioResources* 20(3), 8093-8118.

- <https://doi.org/10.15376/biores.20.3.Karuppusamy>
Karuppusamy, M., Ramamoorthi, R., Karuppusamy, R., and Navin, M. (2023). "Review on fabrication and applications of jute fiber epoxy composite reinforced bio composite," *Journal of Advanced Mechanical Sciences* 2(3), 76-81.
<https://doi.org/10.5281/zenodo.10251273>
- Kumar, M. A., Reddy, G. R., Reddy, G. H., Reddy, K. H., and Reddy, Y. (2011). "Fabrication and performance of hybrid betel nut (*Areca catechu*), short fiber (*Sansevieria cylindrica*: Agavaceae) epoxy composites," *Journal of Metallurgy and Materials Science* 53(4), 375-386
- Kumar, S., Prasad, L., Patel, V. K., Kumar, V., Kumar, A., and Yadav, A. (2022). "Physico-mechanical properties and Taguchi optimized abrasive wear of alkali treated and fly ash reinforced Himalayan agave fiber polyester composite," *Journal of Natural Fibers* 19(14), 9269-9282. <https://doi.org/10.1080/15440478.2021.1982818>
- Kumar, S., Prasad, L., Patel, V. K., Kumar, V., Kumar, A., Yadav, A., and Winczek, J. (2021). "Physical and mechanical properties of natural leaf fiber-reinforced epoxy polyester composites," *Polymers* 13(9), article 1369.
<https://doi.org/10.3390/polym13091369>
- Kumar, S. S., and Raja, V. M. (2021). "Processing and determination of mechanical properties of Prosopis juliflora bark, banana and coconut fiber reinforced hybrid bio composites for an engineering field," *Composites Science and Technology* 208, article 108695. <https://doi.org/10.1016/j.compscitech.2021.108695>
- Kumar, V. V., Dhanalakshmi, S., Raghunathan, V., Ayyappan, V., Sanjay, M. R., and Siengchin, S. (2024). "Characterization of *Allium sativum* stalk-based biomass for automotive brake pad applications," *Biomass Conversion and Biorefinery* 15, 1-14.
<https://doi.org/10.1007/s13399-024-05590-6>
- Kuriakose Mani, A., Mani, A. Z., Jacob, A. V., Krishnan, A., Paul, A. S., Krishnan, A. V., Palanisamy, S., Kannaiyan, S., and Huang, S.-J. (2025). "Mechanical properties and microstructure of ramie fiber-reinforced natural rubber composites," *Journal of Composites Science* 9(7), article 332. <https://doi.org/10.3390/jcs9070332>
- Madhu, P., Sanjay, M. R., Senthamarai kannan, P., Pradeep, S., Saravanakumar, S. S., and Yogesha, B. (2019). "A review on synthesis and characterization of commercially available natural fibers: Part-I," *Journal of Natural Fibers* 16(8), 1132-1144.
<https://doi.org/10.1080/15440478.2018.1453433>
- Mahalingam, J. (2024). "Mechanical, thermal, and water absorption properties of hybrid short coconut tree primary flower leaf stalk fiber/glass fiber-reinforced unsaturated polyester composites for biomedical applications," *Biomass Conversion and Biorefinery* 14(6), 7543-7554. <https://doi.org/10.1007/s13399-022-02958-4>
- Manickaraj, K., Karuppusamy, R., Vijayaprakash, B., and Sakthivel, K. R. (2024a). "Effect of fiber length on the mechanical properties of unsaturated polyester composites enhanced by chemically modified borassus stalk leaf fiber," in: *International Conference on Recent Advancements in Materials Science and Technology* 81-88. https://doi.org/10.1007/978-3-031-69966-5_8
- Manickaraj, K., Nithyanandhan, T., Sathish, K., Karuppusamy, R., and Sachuthanathan, B. (2024b). "An experimental investigation of volume fraction of natural java jute and sponge gourd fiber reinforced polymer matrix composite," in: *2024 10th International Conference on Advanced Computing and Communication Systems (ICACCS)*, pp. 2373-2378. <https://doi.org/10.1109/ICACCS60874.2024.10717221>
- Manickaraj, K., Ramamoorthi, R., Karuppusamy, R., Sakthivel, K. R., and

- Vijayaprakash, B. (2024c). "A review of natural biofiber-reinforced polymer matrix composites," *Evolutionary Manufacturing, Design and Operational Practices for Resource and Environmental Sustainability* Ch 11, pp. 135-141. <https://doi.org/10.1002/9781394198221.ch11>
- Manickaraj, K., Ramamoorthi, R., Sathish, S., and Johnson Santhosh, A. (2023). "A comparative study on the mechanical properties of African teff and snake grass fiber-reinforced hybrid composites: Effect of bio castor seed shell/glass/SiC fillers," *International Polymer Processing* 38(5), 551-563. <https://doi.org/10.1515/ipp-2023-4343>
- Manickaraj, K., Thirumalaisamy, R., Palanisamy, S., Ayrilmis, N., Massoud, E. E. S., Palaniappan, M., and Sankar, S. L. (2025). "Value-added utilization of agricultural wastes in biocomposite production: Characteristics and applications," *Annals of the New York Academy of Sciences* 1549(1), 72-91. <https://doi.org/10.1111/nyas.15368>
- Mittal, M., and Chaudhary, R. (2018). "Experimental investigation on the mechanical properties and water absorption behavior of randomly oriented short pineapple/coir fiber-reinforced hybrid epoxy composites," *Materials Research Express* 6(1), article 15313. <https://doi.org/10.1088/2053-1591/aae944>
- Mittal, V., Saini, R., and Sinha, S. (2016). "Natural fiber-mediated epoxy composites – A review," *Composites Part B: Engineering* 99, 425-435. <https://doi.org/10.1016/j.compositesb.2016.06.051>
- Mohammed, M., Rahman, R., Mohammed, A. M., Adam, T., Betar, B. O., Osman, A. F., and Dahham, O. S. (2022). "Surface treatment to improve water repellence and compatibility of natural fiber with polymer matrix: Recent advancement," *Polymer Testing* 115, article 107707. <https://doi.org/10.1016/j.polymertesting.2022.107707>
- Nanthakumar, J., Palanisamy, Y., Palanisamy, S., Karuppusamy, M., Raja, R., Abbas, M., Alagarsamy, A., and Rahman, M. Z. (2025). "Eco-friendly synthesis of ZnO nanoparticles using Delonix elata extract with enhanced antibacterial activity," *RSC Advances* 15(46), 39305-39313. <https://doi.org/10.1039/D5RA05208D>
- Natrayan, L., Chinta, N. D., Gogulamudi, B., Swamy Nadh, V., Muthu, G., Kaliappan, S., and Srinivas, C. (2024). "Investigation on mechanical properties of the green synthesis bamboo fiber/eggshell/coconut shell powder-based hybrid biocomposites under NaOH conditions," *Green Processing and Synthesis* 13(1), article 20230185. <https://doi.org/10.1515/gps-2023-0185>
- Nayak, S., Khuntia, S. K., Mohanty, S. D., and Mohapatra, J. (2022). "Investigation and fabrication of thermo-mechanical properties of ceiba pentandra bark fiber/poly (vinyl) alcohol composites for automobile dash board and door panel applications," *Journal of Natural Fibers* 19(2), 450-462. <https://doi.org/10.1080/15440478.2020.1745124>
- Nithyanandhan, T., Manickaraj, K., Sathish, K., Ramachandran, N., and Sachuthanathan, B. (2024). "Effects of palm stalk ash on mechanical properties of al6061 reinforced with graphite by using stir casting process," in: *2024 10th International Conference on Advanced Computing and Communication Systems (ICACCS)*, pp. 2357-2364. <https://doi.org/10.1109/ICACCS60874.2024.10717271>
- Oladele, I. O., Makinde-Isola, B. A., Adediran, A. A., Oladejo, M. O., Owa, A. F., and Olayanju, T. M. A. (2020). "Mechanical and wear behaviour of pulverised poultry eggshell/sisal fiber hybrid reinforced epoxy composites," *Materials Research Express* 7(4), article 45304. <https://doi.org/10.1088/2053-1591/ab8585>
- Palaniappan, M., Palanisamy, S., Khan, R., H. Alrasheedi, N., Tadepalli, S., Murugesan, T. mani, and Santulli, C. (2024a). "Synthesis and suitability characterization of

- microcrystalline cellulose from *Citrus x sinensis* sweet orange peel fruit waste-based biomass for polymer composite applications,” *Journal of Polymer Research* 31(4), article 105. <https://doi.org/10.1007/s10965-024-03946-0>
- Palaniappan, M., Palanisamy, S., Murugesan, T. M., Alrasheedi, N. H., Ataya, S., Tadepalli, S., and Elfar, A. A. (2024b). “Novel *Ficus retusa* L. aerial root fiber: A sustainable alternative for synthetic fibres in polymer composites reinforcement,” *Biomass Conversion and Biorefinery* 15, 1-17. <https://doi.org/10.1007/s13399-024-05495-4>
- Palanisamy, S., Kalimuthu, M., Palaniappan, M., Alavudeen, A., Rajini, N., Santulli, C., Mohammad, F., and Al-Lohedan, H. (2022a). “Characterization of *Acacia caesia* bark fibers (ACBFs),” *Journal of Natural Fibers* 19(15), 10241-10252. <https://doi.org/10.1080/15440478.2021.1993493>
- Palanisamy, S., Kalimuthu, M., Santulli, C., Palaniappan, M., Nagarajan, R., and Fragassa, C. (2023). “Tailoring epoxy composites with acacia caesia bark fibers: Evaluating the effects of fiber amount and length on material characteristics,” *Fibers* 11(7), article 63. <https://doi.org/10.3390/fib11070063>
- Palanisamy, S., Mayandi, K., Dharmalingam, S., Rajini, N., Santulli, C., Mohammad, F., and Al-Lohedan, H. A. (2022b). “Tensile Properties and fracture morphology of *Acacia caesia* bark fibers treated with different alkali concentrations,” *Journal of Natural Fibers* 19(15), 11258-11269. <https://doi.org/10.1080/15440478.2021.2022562>
- Pandiarajan, P., Baskaran, P. G., Palanisamy, S., Karuppusamy, M., Marimuthu, K., Rajan, A., Almansour, M. I., Ma, Q., and Al-Farraj, S. A. (2025). “Enhancing polyester composites with nano aristida hystrix fibers: mechanical and microstructural insights,” *BioResources* 20(4), 9257-9281. <https://doi.org/10.15376/biores.20.4.9257-9281>
- Prasad, L., Kapri, P., Patel, R. V., Yadav, A., and Winczek, J. (2023). “Physical and mechanical behavior of ramie and glass fiber reinforced epoxy resin-based hybrid composites,” *Journal of Natural Fibers* 20(2), 1-13. <https://doi.org/10.1080/15440478.2023.2234080>
- Praveen Kumar, A., and Nalla Mohamed, M. (2018). “A comparative analysis on tensile strength of dry and moisture absorbed hybrid kenaf/glass polymer composites,” *Journal of Industrial Textiles* 47(8), 2050-2073. <https://doi.org/10.1177/1528083717720203>
- Praveena, B. A., Buradi, A., Santhosh, N., Vasu, V. K., Hatgundi, J., and Huliya, D. (2022). “Study on characterization of mechanical, thermal properties, machinability and biodegradability of natural fiber reinforced polymer composites and its applications, recent developments and future potentials: A comprehensive review,” *Materials Today: Proceedings* 52, 1255-1259. <https://doi.org/10.1016/j.matpr.2021.11.049>
- Ramasubbu, R., Kayambu, A., Palanisamy, S., and Ayrilmis, N. (2024). “Mechanical properties of epoxy composites reinforced with areca catechu fibers containing silicon carbide,” *BioResources* 19(2), 2353-2370. <https://doi.org/10.15376/biores.19.2.2353-2370>
- Ramesh, M., Tamil Selvan, M., Felix Sahayaraj, A., Jenish, I., Balakrishnan, P., and Ravanan, A. (2023). “Investigation of mechanical and viscoelastic properties of Agave cantala fiber-reinforced green composites for structural applications,” *Proceedings of the Institution of Mechanical Engineers, Part E: Journal of Process*

- Mechanical Engineering*, 09544089231190225.
<https://doi.org/10.1177/09544089231190225>
- Ramesh, M., Tamil Selvan, M., Felix Sahayaraj, A., Jenish, I., Balakrishnan, P., and Ravanan, A. (2025). "Investigation of mechanical and viscoelastic properties of Agave cantala fiber-reinforced green composites for structural applications," *Proceedings of the Institution of Mechanical Engineers, Part E: Journal of Process Mechanical Engineering* 239(3), 1353-1363.
<https://doi.org/10.1177/09544089231190225>
- Rangappa, S. M., Siengchin, S., Parameswaranpillai, J., Jawaid, M., and Ozbakkaloglu, T. (2022). "Lignocellulosic fiber reinforced composites: Progress, performance, properties, applications, and future perspectives," *Polymer Composites* 43(2), 645-691. <https://doi.org/10.1002/pc.26413>
- Ravichandran, G., Ramasamy, K., Manickaraj, K., Kalidas, S., Jayamani, M., Mausam, K., Palanisamy, S., Ma, Q., and Al-Farraj, S. A. (2025). "Effect of Sal wood and babool sawdust fillers on the mechanical properties of snake grass fiber-reinforced polyester composites," *BioResources* 20(4), 8674-8694.
<https://doi.org/10.15376/biores.20.4.8674-8694>
- Sathish, S., Kumaresan, K., Prabhu, L., and Vigneshkumar, N. (2017). "Experimental investigation on volume fraction of mechanical and physical properties of flax and bamboo fibers reinforced hybrid epoxy composites," *Polymers and Polymer Composites* 25(3), 229-236. <https://doi.org/10.1177/096739111702500309>
- Sathishkumar, T. P., Naveen, J. and, and Satheeshkumar, S. (2014). "Hybrid fiber reinforced polymer composites – A review," *Journal of Reinforced Plastics and Composites* 33(5), 454-471. <https://doi.org/10.1177/0731684413516393>
- Stevens, S., Dhas, J. E. R., Lewise, K. A. S., Mohammad, A., and Fahad, M. (2022). "Investigations on chemical behaviours on mechanical properties of natural fiber composites: An evaluation," *Materials Today: Proceedings* 64, 410-415.
<https://doi.org/10.1016/j.matpr.2022.04.761>
- Sumesh, K. R., Ajithram, A., Palanisamy, S., and Kavimani, V. (2024). "Mechanical properties of ramie/flax hybrid natural fiber composites under different conditions," *Biomass Conversion and Biorefinery* 14(23), 29579-29590.
<https://doi.org/10.1007/s13399-023-04628-5>
- Sumesh, K. R., Kavimani, V., Rajeshkumar, G., Indran, S., and Saikrishnan, G. (2021). "Effect of banana, pineapple and coir fly ash filled with hybrid fiber epoxy based composites for mechanical and morphological study," *Journal of Material Cycles and Waste Management* 23(4), 1277-1288. <https://doi.org/10.1007/s10163-021-01196-6>
- Thangavel, N., Shanmugavel, N. K., Karuppusamy, M., and Thirumalaisamy, R. (2024). "Friction and wear behavior of premixed reinforcement hybrid composite materials," *Matéria (Rio de Janeiro)* 29(4), article e20240552. <https://doi.org/10.1590/1517-7076-RMAT-2024-0552>
- Thirumalaisamy, R., Senthil Kumar, S., Chelladurai, S. J. S., Gnanasekaran, S., Sivananthan, S., Geetha, N. K., Ramesh, A., and Assefa, G. B. (2023). "Study on water absorption characteristics, various chemical treatments, and applications of biological fiber-reinforced polymer matrix composites," *Journal of Nanomaterials* 2023(1), article 9903119. <https://doi.org/10.1155/2023/9903119>
- Venkateshwaran, N., ElayaPerumal, A., Alavudeen, A., and Thiruchitrabalam, M. (2011). "Mechanical and water absorption behaviour of banana/sisal reinforced hybrid composites," *Materials and Design* 32(7), 4017-4021.

<https://doi.org/10.1016/j.matdes.2011.03.002>

Vigneshwaran, S., Sundarakannan, R., John, K. M., Johnson, R. D. J., Prasath, K. A., Ajith, S., Arumugaprabu, V., and Uthayakumar, M. (2020). "Recent advancement in the natural fiber polymer composites: A comprehensive review," *Journal of Cleaner Production* 277, article 124109. <https://doi.org/10.1016/j.jclepro.2020.124109>

Vijay, R., and Singaravelu, D. L. (2016). "Experimental investigation on the mechanical properties of Cyperus pangorei fibers and jute fiber-based natural fiber composites," *International Journal of Polymer Analysis and Characterization* 21(7), 617-627. <https://doi.org/10.1080/1023666X.2016.1192354>

Yawas, D. S., Aku, S. Y., and Amaren, S. G. (2016). "Morphology and properties of periwinkle shell asbestos-free brake pad," *Journal of King Saud University - Engineering Sciences* 28(1), 103-109. <https://doi.org/10.1016/j.jksues.2013.11.002>

Article submitted: December 13, 2025; Peer review completed: January 31, 2026;
Revised version received: February 28, 2026; Accepted: May 9, 2026; Published: May 20, 2026.

DOI: 10.15376/biores.21.3.6174-6202